

People's Democratic Republic of Algeria
Ministry of Higher Education and Scientific Research
University M'Hamed BOUGARA – Boumerdes



Institute of Electrical and Electronic Engineering
Department of Power and Control

Final Year Project Report Presented in Partial Fulfilment of
the Requirements for the Degree of
MASTER

In Power Engineering
Option: Power Engineering

Title:

Detection and Classification of Faults in Photovoltaic Modules
Presented by:

- **Mekhalif Ibtihel**

Supervisor:

Pr.Kheldoun Aissa

Registration Number/2024

Abstract:

Solar photovoltaic systems are being widely used in green energy harvesting recently. At the same rate of growth, the modules that come to the end of life are growing fast. Therefore, rapid fault detection and classification of PV modules can help to increase the reliability of the PV systems and reduce operating costs. Inspection and maintenance of solar modules are important to increase the lifetime, reduce energy loss, and environmental protection. A combination of infrared thermography and machine learning methods has been proven effective in the automatic detection of faults in large-scale PV plants. However, so far, few studies have assessed the challenges and efficiency of these methods applied to the classification of different defect classes in PV modules. In this dissertation, an efficient PV fault detection and classification method is proposed to classify different types of PV module anomalies using thermographic images utilizing convolutional neural networks (CNN) and artificial neural networks (ANN). Eleven types of PV module faults such as cracking, diode, hot spot, offline module, and other faults are utilized. Several evaluation metrics were used to assess the performance namely accuracy, recall, precision, and F1 score. The testing accuracy was obtained as 91% for the detection of anomalies in PV modules and 91% to classify defects for four classes and 73% for twelve classes.

In conclusion, the integration of advanced imaging techniques and machine learning algorithms presents a promising avenue for enhancing the reliability of PV systems. As the demand for clean and sustainable energy continues to grow, such innovations will be instrumental in meeting global energy needs while minimizing environmental impact. The advancements outlined in this thesis represent a significant step forward in the pursuit of more efficient and resilient renewable energy infrastructures.

Dedication

I dedicate this Master's thesis with deep gratitude and appreciation to my loving mother, father, and siblings, whose unwavering support, love, and encouragement have been the foundation of my academic journey. Your belief in my abilities and sacrifices made for my education have shaped me into the individual I am today. This achievement would not have been possible without you

To my friends, thank you for standing by my side throughout the writing process. Your words of encouragement and belief in my capabilities have provided me with the strength to overcome challenges and persevere. Lastly, I express my sincere gratitude to all those who have offered their assistance and support, whether through providing resources, proofreading, or lending a listening ear. Your contributions have lightened my burdens and enriched my work.

Acknowledgment:

I would like to extend my heartfelt gratitude and appreciation to all those who have contributed to the successful completion of my Master's thesis. First and foremost, I am profoundly grateful to the almighty ALLAH for granting me the strength and ability to comprehend, learn, and accomplish this thesis.

I would like to express my deepest thanks to my supervisor, Pr. KHELDOUN.A, for his exceptional guidance, expertise, and unwavering support throughout the entire research process. His invaluable insights and constructive feedback have been pivotal in shaping this thesis.

My gratitude extends to the faculty members and mentors who have provided me with their valuable help and profound knowledge during my academic journey, especially Seyyid ahmed Djellouli for his time and efforts. Their dedication to my growth and development has pushed me to new intellectual heights and expanded my horizons.

I am also immensely grateful to my colleagues and friends who have continuously served as a source of inspiration, motivation, and intellectual exchange. Their engaging discussions, innovative ideas, and constant encouragement have played a significant role in shaping my thesis.

Lastly, I would like to acknowledge the unwavering support of my family and loved ones throughout this journey. Their boundless love, understanding, and encouragement have been my source of strength during the most challenging times.

Once again, I express my sincerest appreciation to all those who have contributed to the completion of my Master's thesis.

Content

List of figures

List of tables

List of Abbreviations

General introduction 1

Chapter 1: Photovoltaic system 2

1.2. Introduction 3

1.3. Photovoltaic cell 3

1.3.1. History of photovoltaic systems 3

1.3.2. The working Principle of a solar cell 4

1.3.3. Main types of PV cells 5

1.4. Module and PV array 6

1.5. PV cell modeling 6

1.5.1. Single Diode Model 6

1.5.2. Double diode model 8

1.6. Types of PV systems 8

1.6.1. The ON-Grid system 9

1.6.2. The OFF-Grid system 9

1.7. Conclusion 10

Chapter 2: Faults in PV modules 11

2.1. Introduction 12

2.2. Defects in PV modules 12

2.2.1. Hotspots 12

2.2.2. Shading and Shadowing 12

2.2.3. Cracking 13

2.2.4. Diode failure 13

2.2.5. Soiling 14

2.2.6. Delamination 14

2.2.7. Snail trails 15

2.2.8. Line to line fault 15

2.2.9. Open circuit fault 16

2.2.10. Ground fault 16

2.2.11. Arc fault 17

2.3.	Fault detection techniques	17
2.3.1.	Visual method	18
2.3.2.	Imaging solutions	18
2.3.3.	Electrical detection methods	19
2.3.4.	Protection Device Based Technique	19
2.3.5.	Machine learning (ML) method	19

2.4.	Conclusion.....	20
------	-----------------	----

Chapter 3 : Deep Learning models21

3.1.	Introduction	22
3.2.	Machine Learning and Deep Learning.....	22
3.2.1.	Machine Learning	22
3.2.2.	Deep learning	23
3.3.	Artificial Neural Networks.....	23
3.3.1.	Artificial Neuron.....	24
3.4.	Neural network training	25
3.4.1.	Loss function	25
3.4.2.	Gradient descent.....	26
3.4.3.	Backward propagation.....	26
3.4.4.	Dropout.....	27
3.4.5.	Batch normalization	27
3.5.	Hyperparameters	27
3.5.1.	Learning rate	28
3.5.2.	Batch size	28
3.5.3.	Epochs	28
3.5.4.	Optimizer.....	28
3.5.5.	Metrics.....	28
3.6.	Activation functions	29
3.6.1.	Sigmoid function	29
3.6.2.	ReLU function.....	30
3.6.3.	Softmax function	31
3.7.	Convolutional neural network.....	31
3.7.1.	Convolutional layer	31
3.7.2.	Pooling layer	32
3.7.3.	Fully connected layer	33
3.8.	Conclusion:.....	33

Chapter 4: Results and Discussion34

4.1.	Introduction	35
------	--------------------	----

4.2.	Data Description.....	35
4.3.	Methodology	37
4.3.1.	Used tools	37
4.3.2.	Evaluation metrics.....	38
4.4.	Binary Classification.....	39
4.4.1.	Data preprocessing	39
4.4.2.	Model description.....	40
4.4.3.	Classification report	41
4.5.	Multi-Class Classification.....	43
4.5.1.	Twelve-Class Classification.....	43
4.5.2.	Four-Class Classification	46
4.6.	Compararison	49
4.7.	Conclusion.....	49
	General Conclusion	50
	References:	51

List of figures

Figure 1.1: Solar Cell.....	3
Figure 1.2: Structure of Conventional Solar Cell.....	4
Figure 1.3: Main Types of PV Modules.....	5
Figure 1.4: Difference between a Solar Cell, Module and an Array.....	6
Figure 1.5: The single diode equivalent circuit model of a solar cell.....	7
Figure 1.6: The two diode equivalent circuit model of a solar cell.....	8
Figure 1.7: ON-Grid system.....	9
Figure 1.8: OFF-Grid system.....	9
Figure 2.1: Hotspot in a PV panel.....	12
Figure 2.2: Partial shading on a solar module.....	13
Figure 2.3: Cracked solar module.....	13
Figure 2.4: Thermography of a solar panel with the bypass diode damage.....	14
Figure 2.5: Soiling on a PV panel.....	14
Figure 2.6: Delamination effect on a PV module.....	15
Figure 2.7: Snail trail effect on a PV module.....	15
Figure 2.8: Schematic diagram of a PV system under a line-line fault.....	16
Figure 2.9: Schematic diagram of a PV system under a line-line and open-circuit faults.....	17
Figure 2.10: Schematic diagram of a PV system under a ground fault.....	17
Figure 2.11: Damaged PV system due to an arc fault.....	17
Figure 2.12: Fault diagnosis of PV systems using infrared thermal imaging cameras.....	18
Figure 2.13: PV module electroluminescence image processing.....	19
Figure 3.1: Working principle of an artificial neuron.....	24
Figure 3.2: Biological and artificial neuron.....	24
Figure 3.3: Gradient descent.....	26
Figure 3.4: Sigmoid function.....	29
Figure 3.5: ReLU activation function plot.....	30
Figure 3.6: Convolutional neural network structure.....	31
Figure 3.7: Example of convolution operation with a kernel size of 3x3.....	32
Figure 4.1: Canonical examples of solar module anomalies observable in infrared	

imagery.....	36
Figure 4.2: Number of images of each class in the Infrared Solar Modules dataset.....	38
Figure 4.3: Confusion Matrix.....	39
Figure 4.4: Accuracy and Loss graphs for binary classification.....	41
Figure 4.5: Confusion matrix of the binary classification.....	42
Figure 4.6: Accuracy and Loss graphs for twelve class classification.....	43
Figure 4.7: Confusion matrix of the twelve class classification.....	44
Figure 4.8: Accuracy and Loss graphs for four class classification.....	47
Figure 4.9: Confusion matrix of the four class classification.....	47

List of Tables

Table 4.1: Description of Classes.....	36
Table 4.2: Selected hyperparameters values for binary classification.....	40
Table 4.3: CNN architecture used in the binary classification of faults in PV modules.....	40
Table 4.4: Performance metrics for the binary classification.....	42
Table 4.5: Selected hyperparameters values for the twelve class classification.....	43
Table 4.6: Performance metrics for the twelve class classification.....	45
Table 4.7: Selected hyperparameters values for the four class classification.....	46
Table 4.8: Performance metrics for the four class classification.....	48

List of Abbreviations

PV	Photovoltaic
CNN	Convolutional Neural Network
ANN	Artificial Neural Network
ML	Machine Learning
I	The output current
I_{ph}	The photo-generated current
I_d	The diode current
I_p	The parallel resistor current
I_s	The reverse saturation current
V	The terminal voltage
R_s	The series resistor
R_p	The parallel resistor
a	The diode ideal factor
V_t	The junction thermal voltage
IR	Infrared
DL	Deep Learning
GD	Gradient Descent
BN	Batch Normalization
Adam	Adaptive Moment Estimation
ReLU	Rectified Linear Unit
TP	True Positives
TN	True Negatives
FP	False Positives
FN	False Negatives

General Introduction

The emergence of sustainable energy technologies has profoundly influenced the course of worldwide energy solutions, with photovoltaic (PV) systems occupying a key role.

The increasing reliance on solar energy, driven by its sustainability and environmental benefits, underscores the need for efficient and reliable PV systems. Photovoltaic systems convert sunlight directly into electricity through the photovoltaic effect, a process first discovered over a century ago. Technological advancements in materials science and engineering have progressively enhanced the efficiency and affordability of these systems, making solar energy a viable alternative to conventional energy sources.

Fault detection and classification in PV modules are critical to maintaining the efficiency and longevity of these systems. As the deployment of solar energy systems expands, so does the necessity for effective maintenance strategies to mitigate faults that can lead to significant energy losses and increased operational costs. This essay addresses the critical need for efficient maintenance and inspection of solar photovoltaic systems as their deployment continues to grow globally. The integration of infrared thermography with machine learning models enables the detection of subtle and complex fault patterns that traditional methods might miss. The proposed methodology not only improves the reliability and performance of PV modules but also reduces downtime and operational costs. By classifying a wide range of faults, from minor cracks to significant hot spots, this research supports the sustainable advancement of solar energy technologies, ensuring a more stable and resilient energy supply. This dissertation is divided into four chapters: Chapter one provides a presentation of the PV system's main components and its operation principle. Chapter two derives into the different fault and malfunctions that may occur in this system and the existing fault detection techniques. Chapter three offers an introduction to the principles and methodologies of deep learning. Chapter four details the experiments conducted on fault detection and classification and discusses the obtained results.

Chapter 1

Photovoltaic Systems

1.1. Introduction

Photovoltaic (PV) systems are at the forefront of renewable energy technology due to the global quest of sustainable energy solutions. An overview of PV systems is given in this chapter, along with a look at their main ideas, parts, and uses in the production of sustainable energy.

Through the process known as the photovoltaic effect, which was first documented more than a century ago, photovoltaic devices directly convert sunlight into electricity. Progress in the fields of materials science and engineering has consistently improved photovoltaic technology, rendering it more cost-effective and widely available. Solar cells, which are semiconductor devices that produce energy when exposed to light, are the fundamental component of photovoltaic systems. These mostly silicon-based cells are essential for utilizing solar energy for a variety of purposes and supporting the worldwide shift to clean and sustainable power production.

1.2. Photovoltaic Cell

A solar cell, also referred to as a photovoltaic cell, is a semiconductor device that converts sunlight directly into electricity through the photovoltaic effect. It typically consists of layers of semiconductor material, such as silicon, which absorb photons from sunlight, generating electron-hole pairs and producing an electric current. [1]



Figure 1.1: Solar cell [1]

1.2.1. History of Photovoltaic Systems

The term photovoltaic effect was first discovered in 1839 by a French scientist Alexandre Edmond Becquerel, who was the first who noticed that certain materials produce electricity when exposed to light [2].

However, the first silicon solar cell was accidentally discovered by Russel Ohl in 1940

, that was proved after more studies that it was not only pure silicon but with some impurities which were giving negative regions (n-type) due to the excess of the electrons, and other positive regions due to the lack of electrons (p-type). The semiconductor revolution in 1950s led to the first efficient solar cell in 1954 and the main commercial use of the new solar cell on a spacecraft was in 1958 until 1970s [3].

1.2.2. The Working Principle of a Solar Cell

A solar cell is a semiconductor device consists of a p-n junction created by an impurity doping. The n-region is created by adding phosphorous atoms which have five outer electrons, one more than silicon atom. The fifth electron is mobile and free, and so in this region of the crystal there are many free negative charges.

Vice versa for the p-region, by doping the crystal with boron atoms which have only three free outer electrons, one is always missing for a complete bounding into the crystal structure. This electron could be borrowed from the neighboring atoms, so the place of the missing electron is shifted. It could also be seen as a hole with a positive charge that is mobile and wandering.

There are much more holes than electrons in the p-region so the electrons are called minority charge carriers there.

Due to the large difference in the concentrations from n-type region towards the p-type region, causes the electric field that is responsible for separating the additional electrons and holes produces when light shines on the cell.

An anti-reflective coating is applied to the exposed side of the cell prevents the light from reflecting [4], as is shown in **Figure 1.2**.

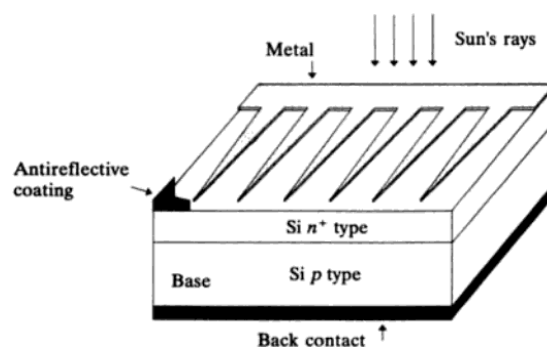


Figure 1.2: Structure of conventional solar cell [4]

1.2.3. Main Types of PV Cells

Photovoltaic (PV) cells serve as the central component of a photovoltaic system. Their primary role is to transform solar light into electrical energy, representing the fundamental function of PV cells within the system.

1.2.3.1. Monocrystalline Solar Cells

Monocrystalline solar cells are made from a single crystal structure, typically silicon. They are known for their high efficiency and uniform appearance. These cells are sliced from a single, pure crystal ingot, making them more efficient in converting sunlight into electricity compared to other types of solar cells, their efficiency stands at around 17% to 22% [5].

1.2.3.2. Polycrystalline Solar Cells

Polycrystalline solar cells are made from silicon material that is melted and poured into molds, then cooled and cut into square-shaped wafers. These cells consist of multiple small silicon crystals, hence the name "polycrystalline." While they are slightly less efficient than monocrystalline cells, they are generally more cost-effective to produce, their efficiency is around 11% to 17% [5].

1.2.3.3. Thin Film Solar Cells

Thin film solar cells are photovoltaic devices made by depositing thin layers of semiconductor materials onto a substrate, like glass or metal. They are lightweight, flexible, and cost-effective, though generally less efficient than traditional silicon-based solar cells, with efficiency ranging from 6% to 11% [5].

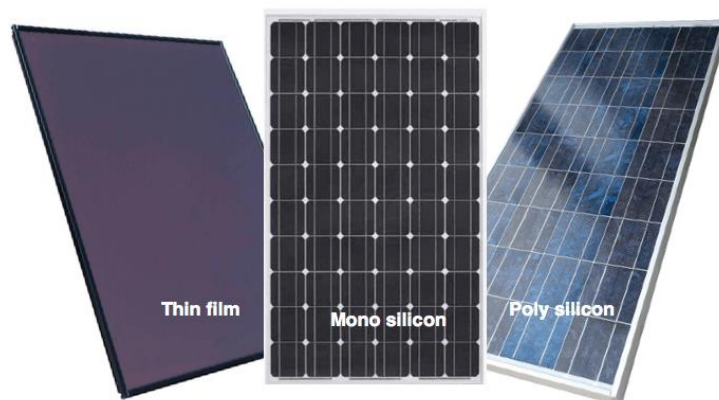


Figure 1.3: Main types of PV modules [5]

1.3. PV Module and Array

A PV module, commonly known as a solar panel, is a collection of solar cells, which generate electricity when exposed to sunlight. These modules are designed to be durable and weather-resistant, typically consisting of multiple solar cells encapsulated within a protective material such as tempered glass and surrounded by a metal frame. PV modules are the basic building blocks of solar photovoltaic systems, and they are interconnected to form larger arrays capable of generating significant amounts of electricity from solar energy [6].

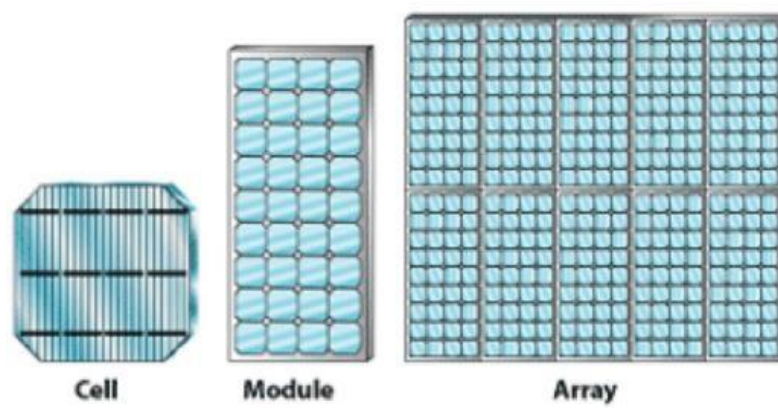


Figure 1.4: Difference between a solar cell, module and an array [6]

1.4. PV Cell Modeling

Understanding the behavior of solar cells is crucial for optimizing their performance and enhancing their efficiency in converting sunlight into electrical energy. To facilitate this understanding, engineers and researchers have developed various mathematical models to describe the electrical characteristics of solar cells under different operating conditions. Two commonly used models are the single diode model and the double diode model [7].

1.4.1. Single Diode Model

The single diode model is a simplified yet effective way to describe the behavior of a solar cell. It assumes that the current-voltage (I-V) characteristic of the solar cell can be modeled using just one diode, along with other parameters:

- **Photocurrent (I_{ph}):** This represents the current generated by the incident light

on the solar cell. It's typically proportional to the intensity of the sunlight.

- **Diode Current (I_d):** Modeled using the Shockley diode equation, this component represents the current flowing through the p-n junction of the solar cell. It's a function of the voltage across the solar cell.
- **Series Resistance (R_s):** This represents the resistance encountered by the current as it flows through the series connection of the solar cell components. It's usually caused by the resistance of the conductive materials and connections within the solar cell.
- **Shunt Resistance (R_{sh}):** This represents the resistance across the solar cell junction, which allows some leakage current to flow. It's essentially the resistance parallel to the solar cell's diode [7].

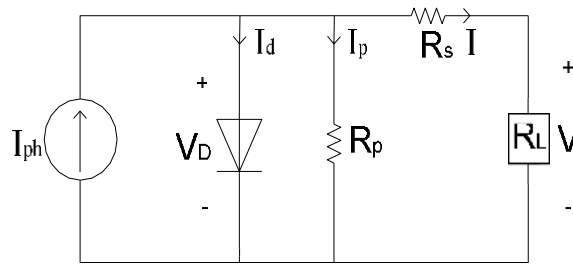


Figure 1.5: The single diode equivalent circuit model of a solar cell [7].

The basic equations expressing the single diode PV cell:

$$I = I_{ph} - I_d - I_p \quad (1.1)$$

$$I_d = I_s \left(e^{\frac{V_D}{aV_t}} - 1 \right) \quad (1.2)$$

$$I_p = \frac{V_D}{R_p} \quad (1.3)$$

$$V_D = V + IR_s \quad (1.4)$$

By substituting (1.2), (1.3) and (1.4) in (1.1) we get:

$$I = I_{ph} - I_s \left(e^{\frac{V + R_s I}{aV_t}} - 1 \right) - \frac{V + R_s I}{R_p} \quad (1.5)$$

1.4.2. Double Diode Model

The double diode model is a more sophisticated representation of solar cell behavior, which accounts for additional mechanisms influencing its performance. This model introduces a second diode component to the single diode model, aiming to capture more accurately the complex behavior of real-world solar cells. The double diode model includes the same parameters as the single diode model but adds another diode equation and its associated parameters [7].

The characteristic equation for two diode model is as given:

$$I = I_{ph} - I_{D1} \left(e^{\frac{V+R_S I}{a1 \cdot V_t}} - 1 \right) - I_{D2} \left(e^{\frac{V+R_S I}{a2 \cdot V_t}} - 1 \right) - \frac{V+R_S I}{R_p} \quad (1.6)$$

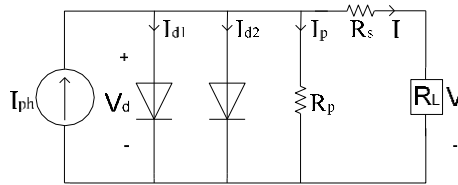


Figure 1.6: The two diode equivalent circuit model of a solar cell [7].

The double diode model offers improved accuracy over the single diode model, especially at higher levels of illumination and with non-ideal operating conditions. However, it also introduces more parameters, which might require more sophisticated measurement techniques for characterization [7].

1.5. Types of PV Systems

Photovoltaic (PV) systems have emerged as a pivotal player in the realm of renewable energy, offering sustainable solutions to meet the growing global demand for electricity. These systems harness the power of sunlight to generate electricity through the photovoltaic effect, converting sunlight directly into usable electrical energy. Among PV systems, two primary setups have become prevalent: on-grid and off-grid systems [8].

1.5.1. The ON-Grid System

An "ON-Grid" solar system is connected to the traditional electrical grid. It generates electricity from sunlight using solar panels and feeds any excess electricity back into the grid. This system relies on the grid for power when solar energy isn't sufficient, such as at night or during cloudy days [8].

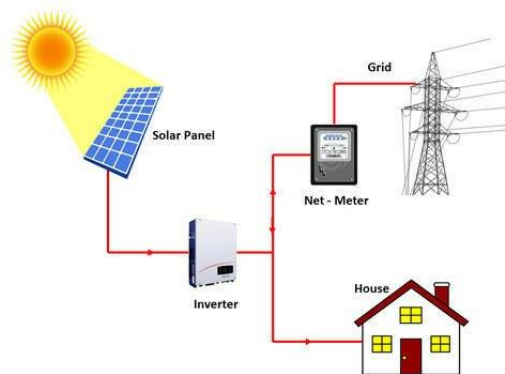


Figure 1.7: ON-Grid System

1.5.2. The OFF-Grid System

An "OFF-Grid" solar system operates independently of the grid. It generates electricity from solar panels and stores excess energy in batteries for use when sunlight isn't available. Off-grid systems are typically used in remote areas where connecting to the grid is impractical or too costly [8].

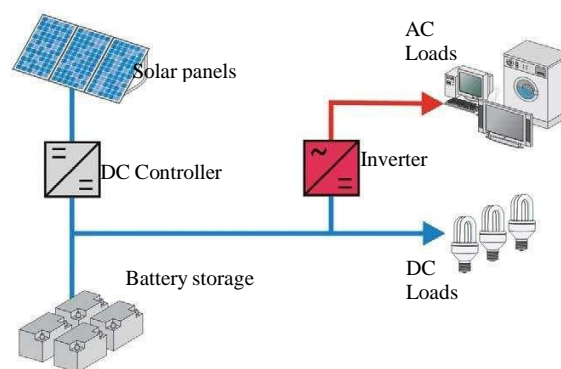


Figure 1.8: Stand-alone Solar System [8].

1.6. Conclusion

This chapter has been devoted to the presentation of PV system's main components. The principle of operation of PV system, whether it is OFF-grid or grid connected, is based on the excitation of the PV cell junction by photons. It is clear that power production is very sensitive to environmental condition. To this, associating PV arrays to power electronic system is necessary to compare their efficiency and quality of generated power.

However, this system is subject to fault. The next chapter will delve into the different faults that may occur in this system.

Chapter 2

Faults in PV Modules

2.1. Introduction

Over the past decade, a rapid growth of photovoltaic technologies and systems have been experienced over the world. The PV is considered as the most promising and major renewable energy source due to providing a clean energy, however it can be affected by many failures and malfunctions that would sap their power.

2.2. Defects in PV Modules

Faults in PV arrays can be classified according to their time characteristic as permanent, incipient, and intermittent. The intermittent defects refer to faults with temporary effect such as shading, dust, snow accumulation, and high humidity. Permanent faults include PV module damages such as short circuit, open-circuit and interconnection damage. On the other hand, partial damage in connections, corrosion, and cell deterioration are the causes of incipient defects. Faults that start out little (incipient) could become permanent ones.

2.2.1. Hotspots

Hotspots happen when certain solar panel cells overheat because of localized shade, dirt, or flaws in the manufacturing process. These hotspots have the potential to lower the panel's overall output and cause irreversible harm to the afflicted cells.

To identify hotspots, thermal imaging is used during the day when the panels are under full sunlight. Areas with noticeably higher temperatures than the rest of the panel will be identified as hotspots [9].



Figure 2.1: Hotspot in a PV panel

2.2.2. Shading and Shadowing

Traditionally, solar panels are connected in a series of parallel ‘strings’. This implies that all of the linked panels in the string will lose power if one panel is shaded by a tree or chimney. This is because the panels are connected in a way that limits the output of each

panel in the system to that of the weakest panel. The output power of a module decreases by half when just one cell in the module is shaded [10].



Figure 2.2: Partial shading on a solar module

2.2.3. Cracking

Cell cracking refers to the development of microcracks in the solar cells within PV modules. Microcracks, also known as microfractures, are tiny cracks in photovoltaic cells. This type of solar degradation is often caused by mechanical stress during installation, transportation, or environmental factors like temperature fluctuations. These microcracks cause reduced panel performance [9].



Figure 2.3: Cracked solar module

2.2.4. Diode Failure

The bypass diode is a key element to ensure the safe operation of PV power plants under inhomogeneous irradiation conditions, namely in the case of partial shading. The reverse current of a diode rises exponentially with its temperature. If a critical temperature is exceeded in reverse bias mode, the power dissipation caused by the reverse current will heat

the diode even further. Consequently, reverse current and power dissipation will rise even more until the diode is destroyed [11].

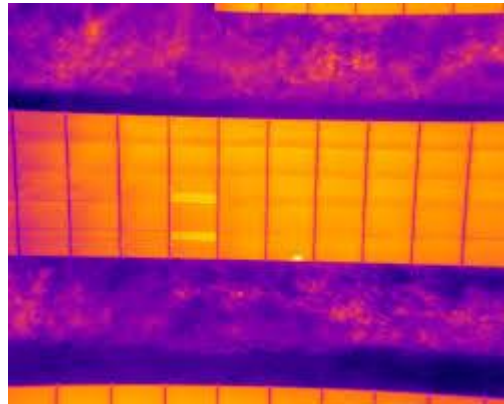


Figure 2.4: Thermography of a solar panel with bypass diode damage

2.2.5. Soiling

Soiling is the accumulation of dirt and debris that build up on the surfaces of PV panels. It negatively affects the performance of PV modules by blocking the irradiance incident onto the PV modules' surfaces; consequently, it lowers the PV array's power production [12].



Figure 2.5: Soiling on a PV module

2.2.6. Delamination

Delamination in PV panels is a serious issue. Delamination can appear in the encapsulant from the front glass, cells or back-sheet. The use of low-cost materials and improper processings are two frequent causes of delamination. It can happen due to moisture entering the backsheet which leads to a reduction in the panel's efficiency [9].



Figure 2.6: Delamination effect on a PV module

2.2.7. Snail Trails

Snail trails also named snail tracks are discolored lines that occurs in the front side metallization of PV cells. They are caused by a chemical reaction within the panel's encapsulation material caused by moisture and oxygen. This chemical reaction leads to a reduction the panel's efficiency [9].



Figure 2.7: Snail trail effect on a PV module

2.2.8. Line to Line fault

A line-to-line fault involves high fault current or DC arcs between two different potential points in the PV array. line-to-line faults are defined as an accidental short-circuiting between two points in the array with different potentials. A line-to-line fault can reverse the current flow through the faulty string. The fault causes a reduction in open-circuit voltage, but short-circuit current may stay the same. The voltage reduction will result in changing the V-I characteristics of the PV array. [13]

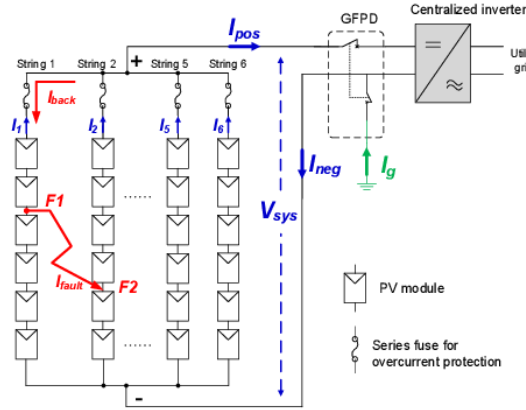


Figure 2.8: Schematic diagram of a PV system under a line-line fault

2.2.9. Open Circuit Fault

An open-circuit fault is an accidental disconnection at a normal conductor during operation. Short circuit current and maximum power are decreased due to the open-circuit fault, while open voltage stays the same [13].

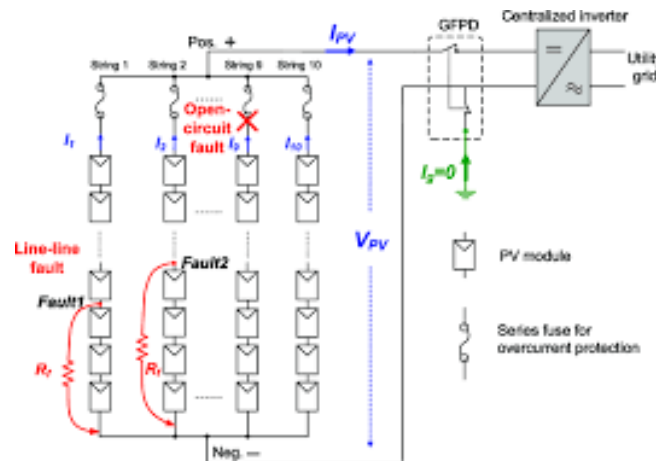


Figure 2.9: Schematic diagram of a PV system under a line-line and open-circuit faults

2.2.10. Ground Fault

A ground fault happens due to unexpected short-circuited path involving one or more carrying current conductors and the ground, which would cause a huge increase in the current passing through the affected conductors causing mismatched currents and changes of the PV array configuration. Several potential reasons for ground faults:

1. cable insulation damage during the installation, due to aging, impact damage, water leakage, and corrosion
2. ground fault within the PV modules
3. insulation damage of cables due to chewing done by rodents

4. accidental short circuit inside the PV combiner box, often at the time of maintenance

Ground fault may result in a number of hazards such as electric shocks and fire hazards [13].

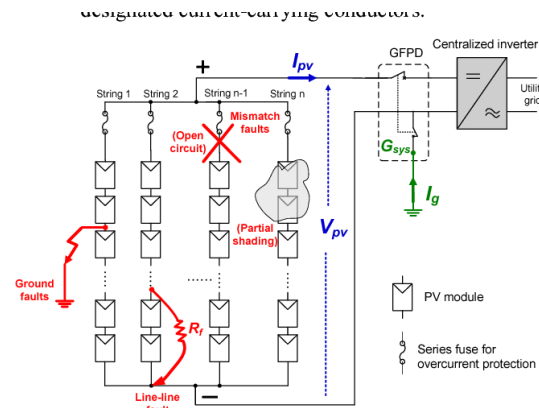


Figure 2.10: Schematic diagram of a PV system under a ground fault

2.2.11. Arc Fault

Arc fault is a result of any intermittent connections including soldered joints and aging of electronic components the chance of its occurrence rises. such faults may produce fire in the PV panels [14].



Figure 2.11: Damaged PV system due to an Arc fault

2.3. Fault detection techniques

PV fault detection techniques enable the location of various PV system problems to be identified. To extend the system's lifespan and ensure safe functioning, such techniques ought to be strong. It is also important for the techniques to identify evolving defects rapidly in order to prevent consequences and additional failures.

2.3.1. Visual Inspection Method

Visual inspections are usually conducted regularly to detect defects in fielded photovoltaic modules. They are the first step in identifying any mechanical or electrical defects and determining whether to carry out additional tests [15].

The major drawback in the visual inspection of PV cells is that it depends on human capabilities. This task could be sometimes boring and not reliable, as it may take longtime to detect fault.

2.3.2. Imaging Solutions

2.3.2.1. Infrared Imaging

Thermal imaging, often known as infrared (IR), is an efficient way to identify defects in solar cells. An IR camera is used to scan the PV array while it is operating. The camera records variations in temperature in the cells and modules as a result of faults in the wiring or interconnection of the modules, hot spots due to internal short circuits, defective bypass diodes, variations in series resistance, cell mismatch, snail trails, and cell cracks are detected [16].

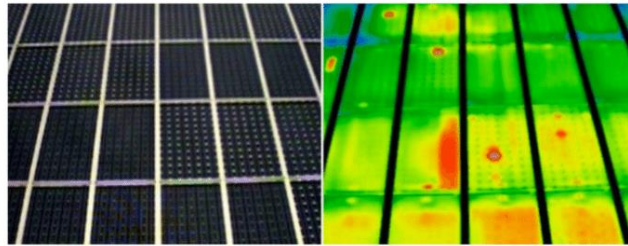


Figure 2.12: Fault diagnosis of PV systems using infrared thermal imaging cameras

2.3.2.2. Ultrasonic Imaging Method

The ultrasonic imaging inspection method is used primarily for detecting cracks before the production of PV modules [16]. It also identifies unbounded cells in a module as well as degradation cracks after PV modules are fielded.

2.3.2.3. Electroluminescence Imaging

This method is utilized for cells and modules defects like cracks, broken gate, and identify solar cells with different conversion efficiency (inhomogeneities). In this method ramped voltage is injected to the module and produce electroluminescence that reveals non-uniformities and defects [16].

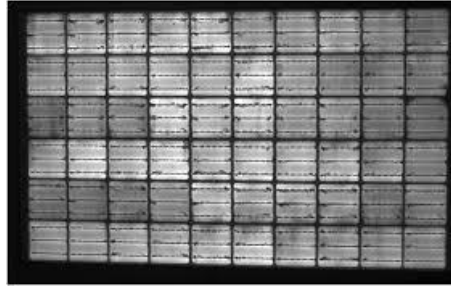


Figure 2.13: PV module Electroluminescence image Processing

2.3.3. Electrical Detection Methods

2.3.3.1. Electrical Current–Voltage (I-V) Measurement Method

The PV string is often the target of the electrical I-V measurement method. The reason for this is that the PV array often has multiple strings connected in parallel at the junction box, enabling the measurement of each string's output separately. string output voltage and current can be measured and checked to identify potential defects like disconnection or degradation in advance. Because such faults reduce string output power or disturb the string I-V curve [17].

2.3.3.2. Power Loss Analysis (PLA) Technique

This method analyzes the PV system's power losses in order to identify and categorize faults. PV system behavior is simulated in real time using climate information data, and parameters that are computed from monitoring data. The monitored data in real work conditions of system DC side are compared with the simulated results to detect system power losses and classify faults [18].

2.3.4. Protection Device Based Technique

PV systems typically have components that may quickly interrupt an electric circuit to stop ongoing defects. When having a ground fault, the PV array is protected by a ground fault detection and interrupt (GFDI) device. When having a line to line and line to ground faults a residual current device (RCD) can be installed to protect PV strings or the entire PV array, it detects the difference in current passing through string terminals or array output terminals, and isolate the string or the array from the system in case the faults happened [19].

2.3.5. Machine Learning (ML) Method

The performance and efficiency of PV cells are subject to various conditions, such as irradiance, temperature, humidity, wind speed, dust, rain, snow, shading... many defects are difficult to define in specific projects. Machine learning techniques can overcome these difficulties very well due to their self-learning nature, making them widely used in this type of

detection [16].

2.4. Conclusion

This chapter introduced faults (defects) in PV solar modules, their causes and how they can affect our systems and finally the faults detection techniques including visual method, imaging techniques, electrical detection methods, machine learning technique and protection device based technique.

Chapter 3

Deep Learning Models

3.1. Introduction

In this chapter, we undertake a methodical investigation into deep learning, an essential element in contemporary artificial intelligence research. Our aim is to offer a thorough introduction to the principles and methodologies of deep learning pertinent to this thesis. Through a systematic approach, we seek to clarify the foundational concepts, trace its historical development, and outline its practical significance.

3.2. Machine Learning and Deep Learning

3.2.1. Machine Learning

Within the field of artificial intelligence (AI), machine learning allows computer systems to automatically gain experience and improve their performance on a given task. Large volumes of data are fed into algorithms to enable them to recognize patterns and provide predictions or choices without needing to be specifically trained to do so [20]. Machine learning techniques are crucial to PV module analysis because they can automatically identify, categorize, and forecast faults. Through the use of labeled PV module data during model training, machines can be trained to identify patterns and characteristics linked to various types of anomalies. After analyzing real-time thermographic images of PV modules, these algorithms can determine whether particular faults are present, send out timely alerts, or take the necessary action. Based on the methods and way of learning, machine learning is divided into mainly three types:

- **Supervised Machine Learning**

When a computer is educated with properly "labelled" training data, it can perform supervised learning, which involves the machine making output predictions based on the training data. Given that the data is marked, some input data has already been assigned the appropriate output.

In supervised learning, the training data serve as the supervisor, teaching the machine to accurately predict the output. It uses the same idea that a student would learn under a teacher's guidance [21].

- **Unsupervised Machine Learning**

Unsupervised learning is a machine learning technique in which training datasets are not used to supervise models. Rather, the models themselves extract the insights and latent patterns from the provided data. It is comparable to the process of learning that occurs in the human brain when something is learned [22].

- **Semi Supervised Machine Learning**

Semi-supervised learning builds a bridge between supervised and unsupervised learning methodologies. In semi-supervised learning, a small number of labeled samples are used to train an initial model, which is then repeatedly applied to a larger dataset [23].

3.2.2. Deep Learning

Deep learning is a subset of machine learning that uses artificial neural networks to learn and make decisions based on data. It involves constructing multiple layers of artificial neurons that can extract higher-level features from raw input data, such as images or sound. Deep learning is used in a variety of applications, including image and speech recognition, and natural language processing. DL algorithms can effectively handle the complexity and variability of PV module data. By training deep neural networks on labeled PV module data, the models can learn to automatically recognize and classify different types of anomalies. The multiple layers of the network allow for the extraction of intricate representations, capturing both global and local patterns within the data. This enables deep learning models to detect subtle variations and distinguish between various types of PV module faults with high accuracy.

3.3. Artificial Neural Networks

An artificial neural network (ANN) is a mathematical model that attempts to mimic the architecture and functions of biological neural networks. An artificial neuron is the fundamental building component of any artificial neural network; it is a straightforward mathematical model (function).

Three basic sets of rules—multiplication, summation, and activation—are present in such a model. Each input value is multiplied by its unique weight at the artificial neuron's entry when it is weighted. The sum function, located in the middle of the artificial neuron, adds up all of the weighted inputs plus bias. The sum of the inputs that have been previously weighted and the bias

are sent through the activation function, also known as the transfer function, at the exit of the artificial neuron.

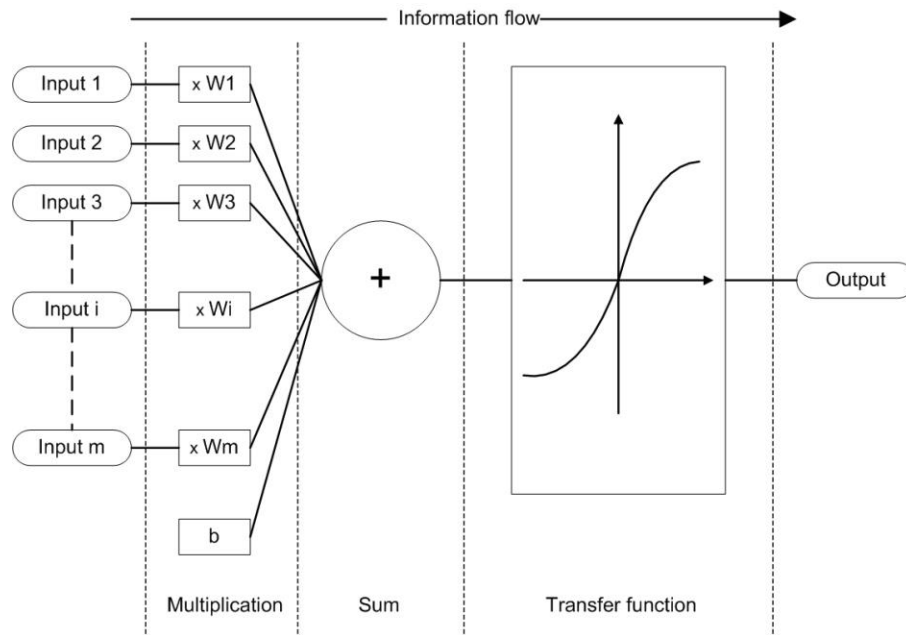


Figure 3.1: Working principle of an artificial neuron.

3.3.1. Artificial Neuron

The fundamental component of each artificial neural network is the artificial neuron. Its structure and operations are based on the study of a biological neuron, which is the fundamental unit of biological neural networks, or systems, that comprise the brain, spinal cord, and peripheral ganglia. **Figure 3.2** illustrates how the left side of a figure depicts a biological neuron with its soma, dendrites, and axon, and the right side of a figure represents an artificial neuron with its inputs, weights, transfer function, bias, and outputs. These similarities in design and functionality can be seen [24].

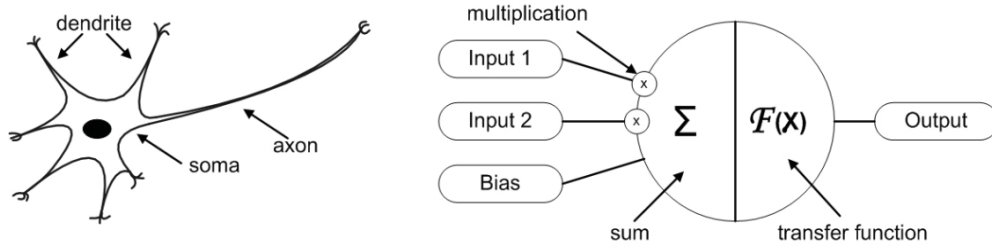


Figure 3.2: Biological and Artificial Neuron design.

In case of biological neuron information enters by its dendrite, is processed by the soma, and then is transferred via an axon. When it comes to artificial neurons, data enters their bodies through weighted inputs (each input has the potential to be amplified by a weight on its own). The body of an artificial neuron then sums the weighted inputs, bias and “processes” the sum with a transfer function. The information that has been processed is finally sent via output(s) by the artificial neuron. The following mathematical explanation demonstrates the benefit of the artificial neuron model's simplicity: [24]

$$y(k) = f\left(\sum_{i=0}^m w_i(k) \cdot x_i(k) + b\right) \quad (3.1)$$

Where:

- $x_i(k)$ is input value in discrete time k for $i = 0, \dots, m$.
- $w_i(k)$ is weight value in discrete time k for $i = 0, \dots, m$.
- b is bias,
- F is a transfer function,
- $y(k)$ is output value in discrete time k for $i = 0, \dots, m$.

3.4. Neural Network Training

In machine learning research, training neural networks is an essential phase. Gradient descent and other error minimization techniques must be used to iteratively optimize the network parameters. Neural networks Training allows them to catch detailed patterns from large datasets, improving their capacity to generalize and generate accurate predictions across a wide range of applications such as computer vision, natural language processing, and reinforcement learning.

3.4.1. Loss Function

When deep learning models are trained, we feed data to the network, generate predictions, compare them with the actual values (the targets) and then compute the loss. In essence, this loss indicates how well the network works overall; the larger it is, the poorer the network performs [25]. The Binary Crossentropy function was used in the binary classification and for the multi-class classifications the Categorical Crossentropy function was used.

3.4.2. Gradient Descent

When training a neural network-based model, Gradient Descent (GD) is a popular optimization algorithm used in machine learning and deep learning that minimizes the cost function of the model. It does this by iteratively changing the model's weights or parameters in the direction of the loss function's negative gradient until the minimum is reached.

The learning happens during the backpropagation while training the neural network-based model [26].

3.4.3. Backward Propagation

The primary strategy for training neural networks is called backpropagation, or backward propagation of mistakes, and it is combined with gradient descent optimization techniques.

The technique uses the current parameters to calculate the network's predictions during the forward pass. As a result, after being fed into the loss function, the predictions are compared against the corresponding ground truth labels.

The model updates the parameters by taking a step of size η in the direction of minimized loss after computing the gradient of the loss function with respect to the current parameters during the backward pass [27].

The gradients (∇) of the loss function (L) with respect to the parameters (θ) are computed mathematically during back propagation as follows:

$$\nabla = \frac{dL}{d\theta} \quad (3.2)$$

These gradients are then used to update the parameters in the opposite direction of the gradient as shown in **Figure 3.3**:

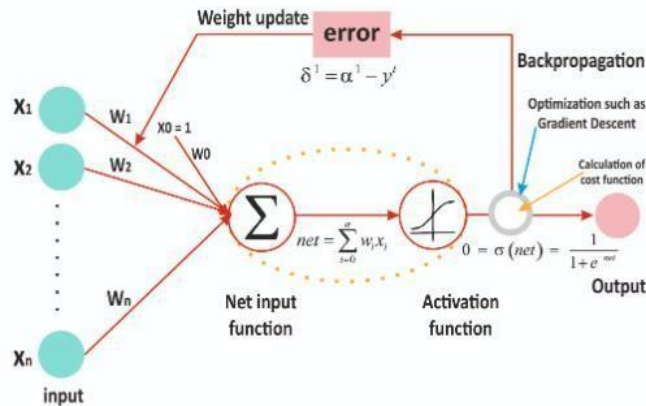


Figure 3.3: Gradient descent and weights update in backpropagation algorithm [28].

3.4.4. Dropout

Dropout is a regularization technique that is frequently used in deep learning models to prevent overfitting. During training, it randomly removes (sets to zero) a certain number of neurons from the neural network. This prevents the network from being overly dependent on any specific features or neurons, and forces it to learn more reliable ones by promoting better generalization to unseen data. dropout is a popular method for improving the robustness and performance of deep neural networks in a variety of applications [28].

3.4.5. Batch Normalization

Batch normalization is a technique for training deep neural networks that standardizes the inputs to mini-batch layers. This process has the effect of stabilizing the learning process and reduces the number of training epochs significantly. By using BN, the CNN model performs better, has a faster training rate, and is less sensitive to the weight initialization. Additionally, it functions as a regularizer by lessening over-fitting and enhancing the network's generalization capabilities [29].

3.5. Hyperparameters

Neural networks have a large number of hyperparameters such as the learning rate, the rate of regularization, and so on. The term "hyperparameter" is used to specifically refer to the parameters regulating the design of the model (like learning rate and regularization), and they are different from the more fundamental parameters representing the weights of connections in the neural network [30].

3.5.1. Learning Rate

The learning rate is a hyperparameter that controls the magnitude of parameter changes during training. It controls how much to update the weights with respect to the loss gradient. A high learning rate means you are taking large steps, which might cause you to overshoot the minimum. On the other hand, a low learning rate means smaller steps, which can lead to slow convergence or getting stuck in a local minimum [31].

3.5.2. Batch Size

Batch size represents the number of samples used in one forward and backward pass through the network and has a direct impact on the accuracy and computational efficiency of the training process. One way to understand the batch size is as a trade-off between speed and accuracy. While smaller batch sizes can yield better accuracy but can be more computationally expensive and time-consuming, larger batch sizes can result in faster training durations but may also cause lower accuracy and overfitting [32].

3.5.3. Epochs

An epoch is a full training cycle that goes through every sample in the training dataset. The number of epochs determines how many times the model will see the entire training data before completing training.

The number of epochs is a crucial hyperparameter to set accurately because it can impact the accuracy and computational efficiency of the training process. If the number of epochs is set too small, the model may not learn the underlying patterns in the data, which could lead to underfitting; on the other hand, if the number of epochs is set too large, the model may overfit the training data, which could result in suboptimal generalization performance on new, unseen data [32].

3.5.4. Optimizer

The optimizers determine the way the model makes updates to the network weights and the learning rate with an aim to reduce the errors and losses. The optimization algorithms are greatly responsible for reducing the errors as well as the losses and, consequently, provide much more accurate results. I have used an Adam Adaptive Moment Estimation optimizer (Adam) for my experiment and it is used for optimizing the gradient descent [33].

3.5.5. Evaluation Metrics

Evaluation metrics are used to measure the quality of the machine learning model. Evaluating machine learning models is essential for any project. There are various model evaluation metrics available to test a model. These include classification accuracy, logarithmic loss, confusion matrix, and others. Classification accuracy is the ratio of the number of correct predictions to the total number of input samples, which is usually what we refer to when we use the term accuracy. [34]

3.6. Activation Functions

Activation functions or non-linear functions have degree more than one and have a curvature when plotted. If an activation function is not used in a neural network then the output signal would simply be a simple linear combination of the output. A neuron without an activation functions acts as a linear regression model with limited performance and power most of the times.

Thus, we need to apply an activation function to make the network dynamic with the ability to extract complex and complicated information from data and represent nonlinear convoluted random functional mappings between input and output [35].

Applying an activation function to the weighted sum of a neuron's inputs, which includes the bias term, yields the neuron's activity as shown below:

$$y = f(w_1x_1 + W_2x_2 + \dots + w_nx_n + b) \quad (3.3)$$

Such that:

- y: output of the neuron.
- f: activation function.
- w: weight.
- x_i : features.
- b: bias.

3.6.1. Sigmoid Function

It is the most widely used activation function as it is a non-linear function. Sigmoid function transforms the values in the range 0 to 1. It can be defined as:

$$f(x) = \frac{1}{1 + e^{-x}} \quad (3.4)$$

Sigmoid function is continuously differentiable S-shaped function [35].

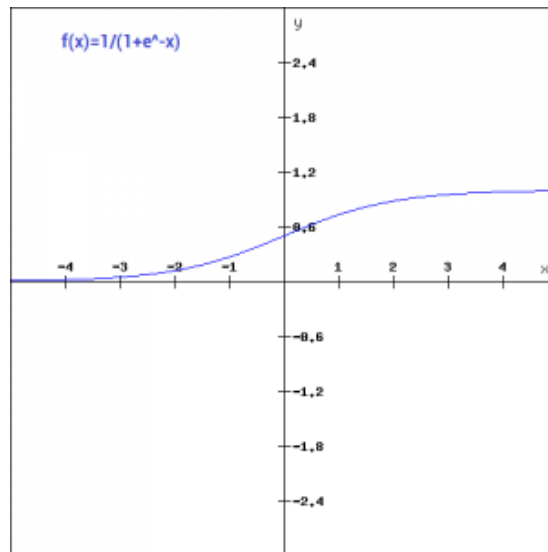


Figure 3.4: Sigmoid Function

3.6.2. Rectified Linear Unit (ReLU) Function

ReLU stands for rectified linear unit and is a non-linear activation function which is widely used in neural network.

It is more efficient than other functions because as all the neurons are not activated at the same time, rather a certain number of neurons are activated at a time [35]. It can be defined mathematically as:

$$f(x) = \max(0, x) \quad (3.5)$$

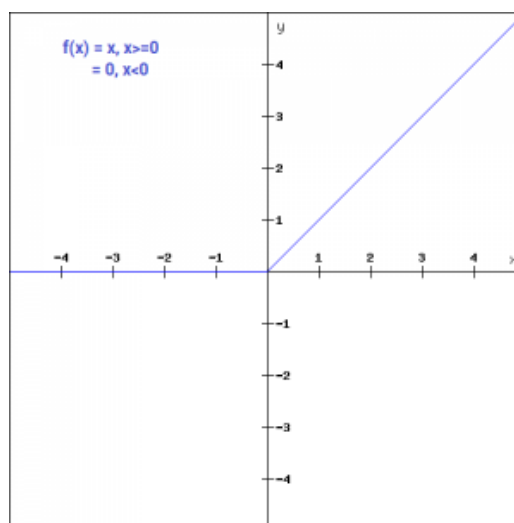


Figure 3.5: ReLU Activation Function plot

3.6.3. Softmax Function

Softmax function is a combination of multiple sigmoid functions. Unlike sigmoid functions which are used for binary classification, softmax function can be used for multiclass classification problems [35]. It can be expressed as:

$$f(x) = \frac{e^{x_i}}{\sum_{j=1}^k e^{x_j}} \quad (3.6)$$

3.7. Convolutional Neural Network

Convolutional Neural Networks are very similar to ordinary neural networks from the previous chapter: they are made up of neurons that have learnable weights and biases. Each neuron receives some inputs, performs a dot product and optionally follows it with a non-linearity. The whole network still expresses a single differentiable score function: from the raw image pixels on one end to class scores at the other. And they still have a loss function on the last (fully connected) layer and all the tips we developed for learning regular Neural Networks still apply. CNN architectures make the explicit assumption that the inputs are images, which allows us to encode certain properties into the architecture. These then make the forward function more efficient to implement and vastly reduce the amount of parameters in the network [36]. The CNN architecture includes several building blocks, such as convolution layers, pooling layers, and fully connected layers. A typical architecture consists of repetitions of a stack of several convolution layers and a pooling layer, followed by one or more fully connected layers.

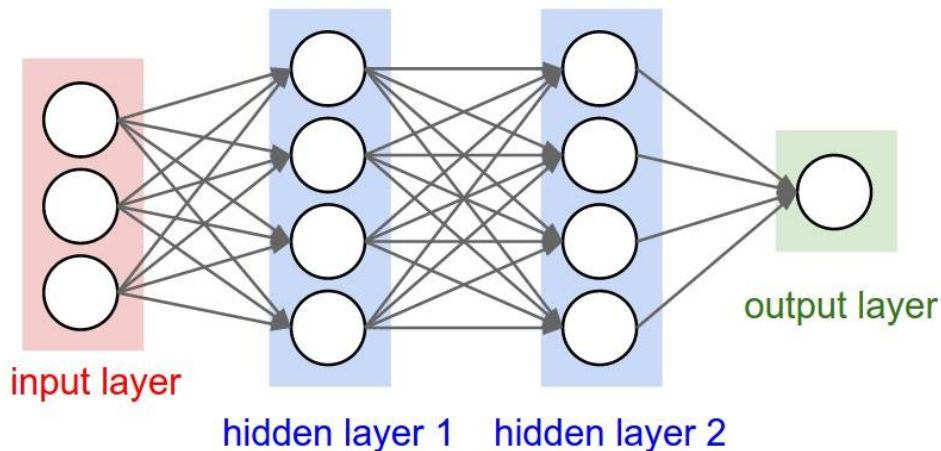


Figure 3.6: Convolutional Neural Network structure

3.7.1. Convolutional Layer

A convolution layer is a fundamental component of the CNN architecture that performs feature extraction, which typically consists of a combination of linear and nonlinear operations, i.e., convolution operation and activation function. Convolution is a specialized type of linear operation used for feature extraction, where a small array of numbers, called a kernel, is applied across the input, which is an array of numbers, called a tensor. An element-wise product between each element of the kernel and the input tensor is calculated at each location of the tensor and summed to obtain the output value in the corresponding position of the output tensor, called a feature map. This procedure is repeated applying multiple kernels to form an arbitrary number of feature maps, which represent different characteristics of the input tensors; different kernels can, thus, be considered as different feature extractors. Two key hyperparameters that define the convolution operation are size and number of kernels (Filters) [37].

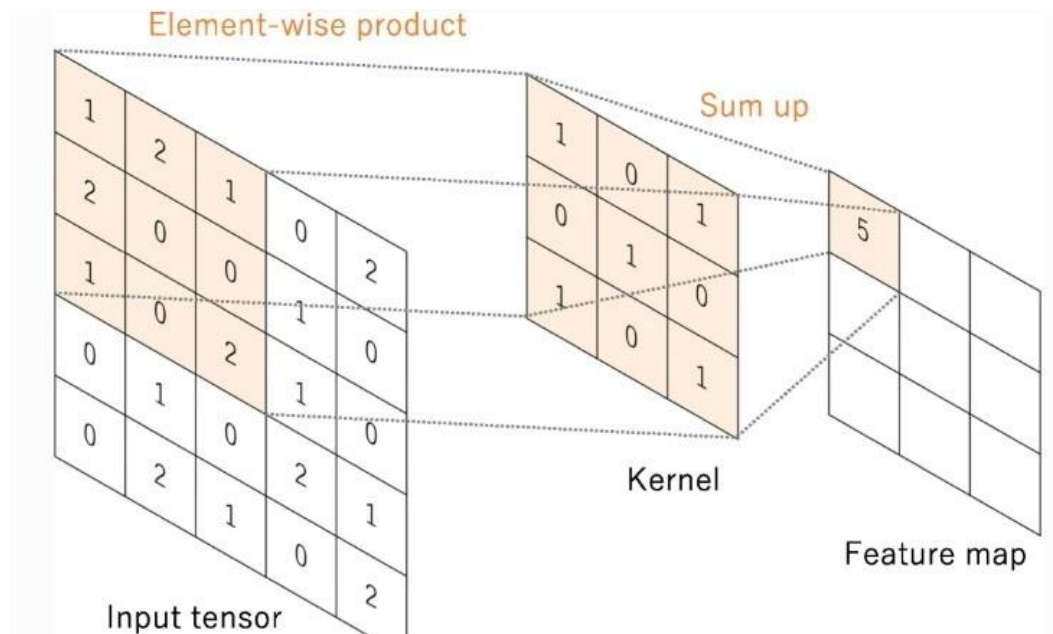


Figure 3.7: Example of convolution operation with a kernel size of 3×3

3.7.2. Pooling Layer

A pooling layer is another building block of a CNN. Its function is to progressively reduce the spatial size of the representation to reduce the amount of parameters and computation in the network. Pooling layer operates on each feature map independently. The most common approach used in pooling is max pooling. Max pooling is a pooling operation that selects the maximum element from the region of the feature map covered by the filter. Thus, the output after maxpooling layer would be a feature map containing the most prominent features of the previous feature map [38].

3.7.3. Fully Connected Layer

The fully connected layer is an important component in artificial neural networks, especially in feedforward neural networks. It takes input from the final convolutional or pooling layer, which is in the form of a set of metrics (Feature maps) and those metrics are attended to create a vector. This vector is then fed into the fully connected layer to generate the final output of the CNN (classifications) [39].

3.8. Conclusion:

This chapter provided details of background study on deep learning convolutional neural networks and outlined the basic concepts of Convolutional Neural Networks in addition to the advanced techniques to apply for training a deep learning model better.

Chapter 4

Results and Discussion

4.1. Introduction

In this chapter, the outcomes of our comprehensive analysis in the field of PV faults image classification is unveiled. Building upon the foundation laid in the previous chapters where the background of PV defects and deep learning methodologies were explored, and the approach used, this chapter serves as the culmination of the research efforts.

The investigation centers on the utilization of deep neural networks and datasets sourced from Kaggle. This exploration extends to both binary classification and multi-class classification.

The primary objective is to enhance the accuracy of PV fault detection and classification compared to existing deep learning methods.

4.2. Dataset Description

In this work, I used the Infrared Solar Modules dataset that was published in 2020 by Raptor Maps Inc for research community, which includes 20000 infrared images with equal anomaly and no-anomaly classes. Each IR image is 24 by 40 pixels. There are 11 different anomaly classes and one nominal module (No-Anomaly) class. The number of anomaly samples varies from 175 to 1877 images in the dataset. The imbalance of classes in the dataset is a big challenge of the deep learning technique. It is noted that the proportion of the classes in the dataset is according to the total existing global findings. Some PV modules could be easily observed differently, such as Cell vs. Diode or Hot-spot vs. Offline-Module. However, there are challenges to distinguish some classes such as Cell vs. Soiling or Cell-Multi vs. Vegetation. [40]

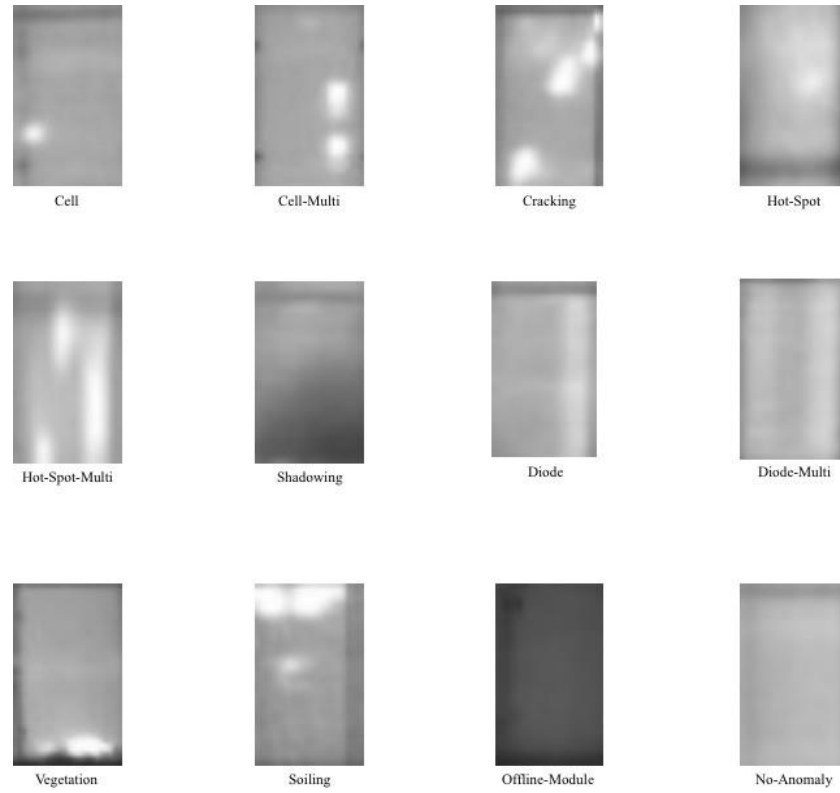


Figure 4.1: Canonical examples of solar module anomalies observable in infrared imagery [40]

Table 4.1: Description of Classes [40]

Class Name	Images	Description
Cell	1,877	Hot spot occurring with square geometry in single cell.
Cell-Multi	1,288	Hot spots occurring with square geometry in multiple cells.
Cracking	941	Module anomaly caused by cracking on module surface.
Hot-Spot	251	Hot spot on a thin film module.
Hot-Spot-Multi	247	Multiple hot spots on a thin film module.
Shadowing	1056	Sunlight obstructed by vegetation, man-made structures, or adjacent rows.
Diode	1,499	Activated bypass diode, typically 1/3 of module.
Diode-Multi	175	Multiple activated bypass diodes, typically affecting 2/3 of module.
Vegetation	1,639	Panels blocked by vegetation.
Soiling	205	Dirt, dust, or other debris on surface of module.
Offline-Module	828	Entire module is heated.
No-Anomaly	10,000	Nominal solar module.

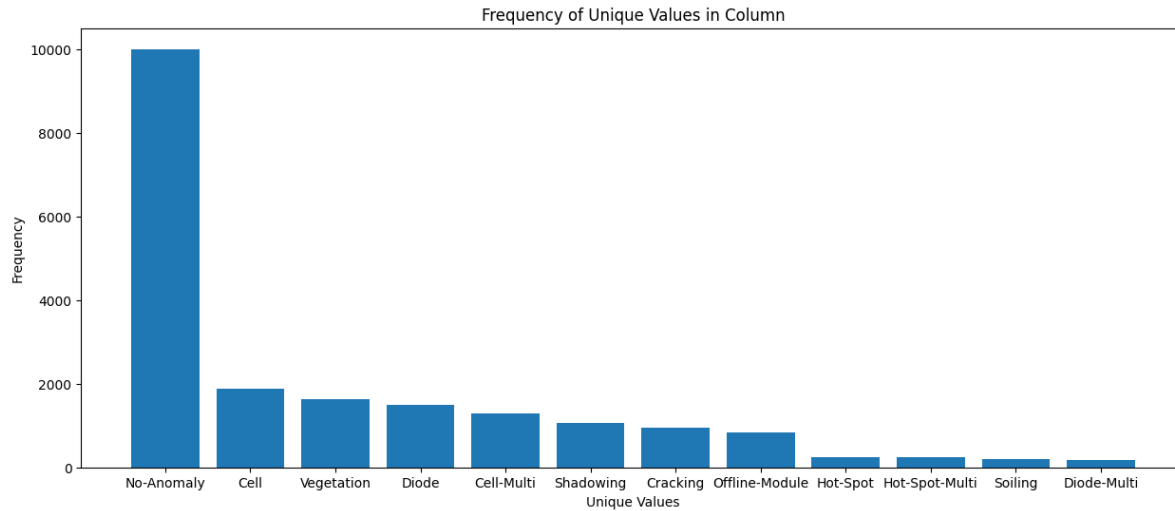


Figure 4.2: Number of images of each class in the Infrared Solar Modules dataset

4.3. Methodology

4.3.1. Used Tools

4.3.1.1. Kaggle

Kaggle is an online community platform for data scientists and machine learning enthusiasts. It provides access to a diverse array of datasets and hosts competitions that challenge data scientists and machine learning enthusiasts to solve real-world problems.

The aim of this online platform is to help professionals and learners reach their goals in their data science journey with the powerful tools and resources it provides [41].

4.3.1.2. Python

Python is an interpreted, object-oriented, high-level programming language with dynamic semantics. Its high-level built in data structures, combined with dynamic typing and dynamic binding, make it very attractive for Rapid Application Development, as well as for use as a scripting or glue language to connect existing components together. Python's simple, easy to learn syntax emphasizes readability and therefore reduces the cost of program maintenance. [42]

4.3.1.3. Tensorflow

TensorFlow [43] is an open-source numerical computing library developed by Google that focuses on machine learning and deep learning applications. It provides an adaptive and fast framework for executing multi-dimensional array-based mathematical computations known as

tensors. TensorFlow is intended to make it easier to construct, train, and deploy machine learning models, particularly neural networks, across a variety of platforms and computing environments.

4.3.1.4. Keras

Keras [44] is a high-level, deep learning API developed by Google for implementing neural networks. It is written in Python and is used to make the implementation of neural networks easy. It also supports multiple back-end neural network computation.

4.3.2. Evaluation Metrics

A metric help in evaluating any designed model's performance. The metrics show how accurate the designed model is. [45] They give a comparison between actual and predicted values as follows:

- **True Positive(TP):** The actual value and the predicted values are the same.
- **True Negative(TN):** The actual value and the predicted values are the same.
- **False Positive(FP):** The actual value is negative, but the model has predicted it as positive.
- **False Negative(FN):** The actual value is positive, but the model has predicted it as negative.

		Actual Values	
		Positive (1)	Negative (0)
Predicted Values	Positive (1)	TP	FP
	Negative (0)	FN	TN

Figure 4.3: Confusion Matrix

4.3.2.1. Accuracy

Accuracy is how close or far off a given set of measurements are to their true value [45].

$$accuracy = \frac{TP+TN}{TP+TN+FP+FN} \quad (4.1)$$

4.3.2.2. Precision

Precision is a statistic for determining the percentage of input data cases that are reported to be true [45].

$$precision = \frac{TP}{TP+FP} \quad (4.2)$$

4.3.2.3. Recall

Indicates the percentage of total relevant results properly classified by the model. [45] It can be calculated using the following formula:

$$recall = \frac{TP}{TP+FN} \quad (4.3)$$

4.3.2.4. F1-Score

The F1-Score is a metric in classification that combines precision and recall scores of a model into a single value. The F1-Score ranges between 0 and 1, with higher values indicating better model performance. [46]

$$F1\ Score = \frac{2 \times (precision \times recall)}{precision + recall} \quad (4.4)$$

4.4. Binary Classification

4.4.1. Data Preprocessing

In this binary classification, the Infrared Solar Modules dataset downloaded from Kaggle was used, the dataset consists of 12 classes one no-anomaly class and 11 anomaly classes. After merging the eleven anomaly classes to get one class (anomaly) the dataset became balanced with 10000 images for each class.

Several combinations of hyperparameter values were carefully evaluated to determine the most successful ones.

After extensive testing the hyperparameters presented in Table 4.2 were chosen. The subsections that follow give thorough results, analyses, and discussions for the model and imaging technique, giving light on their adaptability to different data situations and their implications for practical PV faults picture classification.

Table 4.2: Selected hyperparameters values for binary classification

Hyperparameter	Fixed value
Number of Epochs	80
Learning rate	0.0001
Batch size	32
Optimizer	Adam
Loss function	Binary crossentropy
Metrics	Accuracy

4.4.2. Model Description

The Convolutional Neural Network (CNN) architecture employed in this study comprises multiple layers designed to effectively extract and classify features from input images. The model begins with a convolutional layer with 32 filters of size 3x3, reducing the input dimensions from 40x24 to 38x22 and outputting 32 feature maps, followed by a max pooling layer that further reduces the spatial dimensions to 19x11. This is succeeded by a second convolutional layer with 64 filters, yielding 64 feature maps of size 17x9, and another max pooling layer that reduces the size to 8x4. A third convolutional layer with 64 filters reduces the feature map size to 6x2. The output from these layers is then flattened into a 1D vector of 768 elements, which is passed through a fully connected layer with 64 neurons. A dropout layer is applied to prevent overfitting by randomly dropping 20% of the connections during training. Finally, a dense layer with a single neuron using a sigmoid activation function outputs the probability for binary classification. As shown in **Table 4.3**.

Table 4.3: CNN architecture used in the binary classification of faults in PV modules

Layer (type)	Output Shape	Number of Parameters
conv2d (Conv2D)	(None, 38, 22, 32)	320
max_pooling2d (MaxPooling2D)	(None, 19, 11, 32)	0
conv2d_1 (Conv2D)	(None, 17, 9, 64)	18,496
max_pooling2d_1 (MaxPooling2D)	(None, 8, 4, 64)	0
conv2d_2 (Conv2D)	(None, 6, 2, 64)	36,928
flatten (Flatten)	(None, 768)	0
dense (Dense)	(None, 64)	49,216
dropout (Dropout)	(None, 64)	0
dense_1 (Dense)	(None, 1)	65

4.4.3. Classification Report

As can be seen from **Figure 4.4**, the training and validation accuracy graph exhibit a noticeable upward trend, indicating successful learning progress, while the loss graph indicates a consistent downward trend, indicating effective convergence during training and validation.

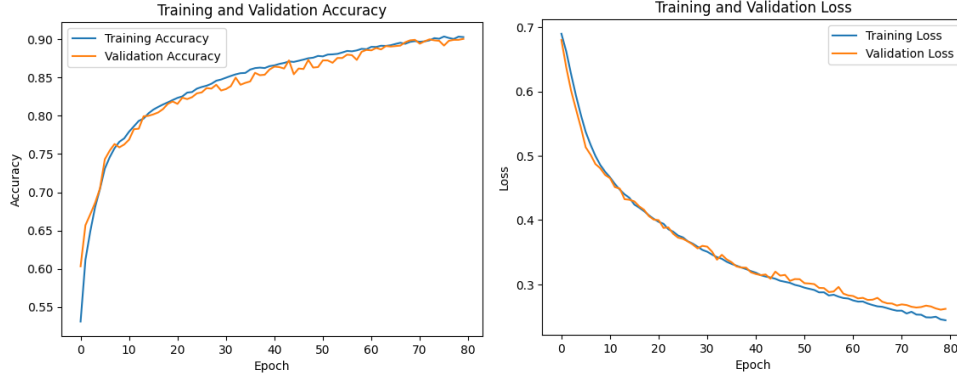


Figure 4.4: Accuracy and Loss graphs for binary classification

Further information is extracted from the confusion matrix in **Figure 4.5:**

As can be noticed, it is easier to detect the No-Anomaly PV modules than the Anomaly PV modules.

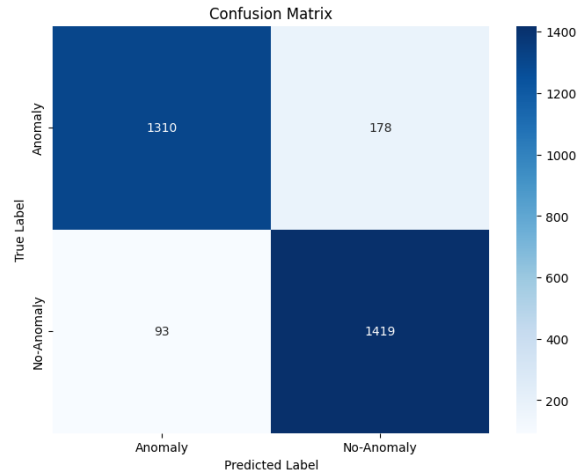


Figure 4.5: Confusion matrix of the binary classification

As we can see from the confusion matrix is giving good results. In addition, other metrics are covered in **Table 4.4:**

Table 4.4: Performance metrics for the binary classification

Class	Precision	F1-Score	Recall	Total accuracy
Anomaly	0.93	0.91	0.88	0.91
No-anomaly	0.89	0.91	0.94	

It shows the performance of the binary classification. Notably, it demonstrated high accuracy at 0.91, indicating satisfactory classification. In particular, the Anomaly class achieved a precision of 0.93, recall of 0.88, and F1-Score of 0.91, showing an outstanding performance in detecting defective PV modules. On the other hand, the Anomaly class achieved a precision of 0.89, recall of 0.94, and F1-Score of 0.91, showing a remarkable performance in detecting the non-defective modules.

4.5. Multi-Class Classification

4.5.1. Twelve-Class Classification

In multi-class classification, the Infrared Solar Modules dataset was used, the dataset consists of 12 classes one no-anomaly class and 11 anomaly classes.

After doing many tests the hyperparameters presented in **Table 4.5** were chosen. The subsections that follow give thorough results, analyses, and discussions for the model and imaging technique.

Table 4.5: Selected hyperparameters values for twelve-class classification

Hyperparameter	Fixed value
Number of Epochs	200
Learning rate	0.0001
Batch size	32
Optimizer	Adam
Loss function	categorical crossentropy
Metrics	Accuracy

4.5.1.1. Classification Report

Using the model architecture described in **Table 4.3** we got the following results seen in **figure 4.6**

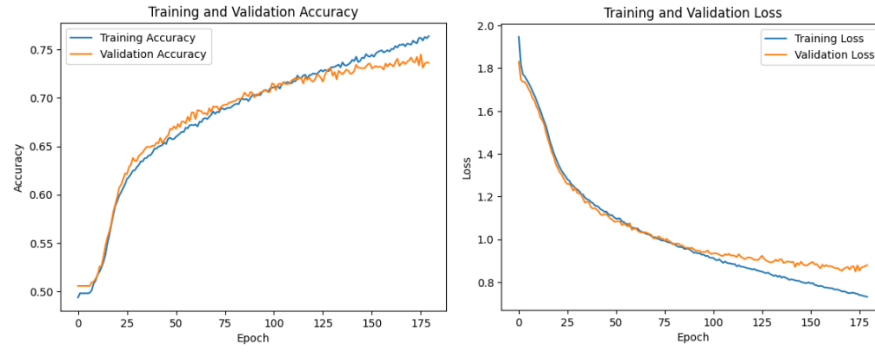


Figure 4.6: Accuracy and Loss graphs for twelve class classification

As can be seen the training and validation accuracy graph exhibit a noticeable upward trend, indicating positive learning progress, while the loss graph indicates a consistent downward trend, indicating effective convergence during training.

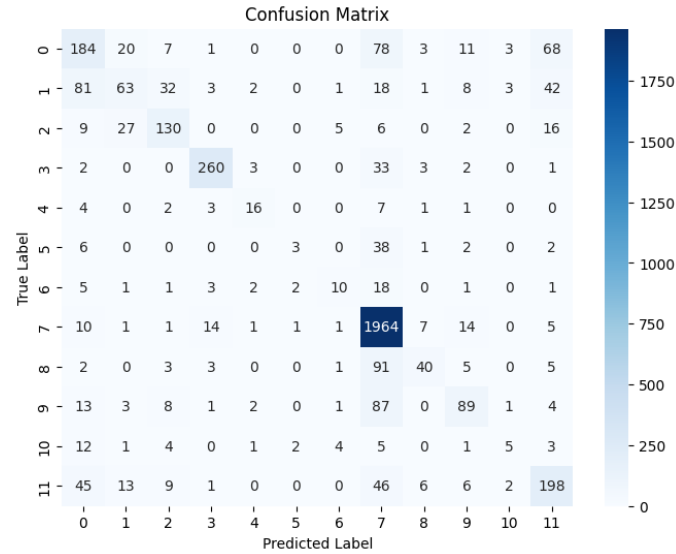


Figure 4.7: Confusion matrix of the twelve class classification

The confusion matrix in **figure 4.7** shows that it is easier to detect the No-Anomaly PV modules than the Anomaly PV modules. The false prediction of the No-Anomaly module is mostly on the Offline-module class. This is reasonable because the all the part in the Offline-module is heated and the entire area will have a similar temperature like a No-Anomaly module.

The Cell, Cell-Multi, and Vegetation modules are the most false prediction on each other. The soiling module is the most difficult to classify, which has missed prediction on many other modules such as Cell, Cell-Multi, Cracking, Hot-Spot-Multi, and Vegetation. The soiling, hot spot, hot-spot-multi modules and diode-multi are the most difficult to classify due to their low number of samples. The other remained modules have the most false-prediction on the No-Anomaly module, this could be because the model was still biased for the No-Anomaly module due to a large number of samples (50% in total) on the No-Anomaly module. The Cell has a spot but it was predicted as a Cell-Multi because it has a long-shape like a merge of two spots.

The Diode, cracking and No-anomaly modules are some of the easiest predicted modules, which have high accuracies of 66%, 90% and 82%, respectively, as shown in **Table 4.6**.

Table 4.6: Performance Metrics for the twelve class classification

Class	precision	Recall	F1-Score	Total Accuracy
Cell	0.49	0.49	0.49	0.74
Cell-Multi	0.49	0.25	0.33	
Cracking	0.66	0.67	0.66	
Diode	0.90	0.86	0.88	
Diode-Multi	0.59	0.47	0.52	
Hot-spot	0.38	0.06	0.10	
Hot-Spot-Multi	0.43	0.23	0.30	
No-Anomaly	0.82	0.97	0.89	
Offline-Module	0.65	0.27	0.38	
Shadowing	0.63	0.43	0.51	
Soiling	0.36	0.13	0.19	
Vegetation	0.57	0.61	0.59	

As it can be seen from **Table 4.6** our model achieved a total accuracy of 74%. The best performance was that of the Diode, Cracking and No-Anomaly modules. It can be noticed that the minority classes (classes that have the least number of samples) which are Hot-spot, Hot-Spot-Multi, Diode-Multi, Cell-Multi and Soiling have the worst accuracy due to their low number

of samples which makes it difficult for the model to learn and perform a correct classification.

Also, the similarity of the IR images makes it difficult for the model to classify the correct anomaly types. It requires additional images for better prediction of the anomalies.

4.5.2. Four-Class Classification

This proposed case evaluates the effect of the elimination of the minority classes on the performance of the model.

4.5.2.1. Data Preprocessing

Based on the results we got from the twelve class classification, it was noticed that the classes with the least number of samples have the lowest accuracy and they affect the total accuracy and efficiency of the classification of PV module faults.

The proposed solution is by merging some cases that have similar features and deleting the minority classes and leaving the classes that have the highest accuracy.

As noticed in **Table 4.6** the Diode, Cracking and No-anomaly modules have high accuracies and by knowing also that Diode and Diode-Multi have almost same features and so is the case for Cell and Cell-Multi modules, it was decided to merge the classes together and delete the minority classes which are Hot-Spot, Hot-Spot-Multi, Soiling, shadowing and vegetation.

Which lead to having a four class classification of the No-Anomaly, Diode, Cracking and Cell.

Several combinations of hyperparameter values were carefully evaluated to determine the most successful ones.

After extensive testing the hyperparameters presented in **Table 4.7** were chosen.

Table 4.7: Selected hyperparameters values for four class classification

Hyperparameter	Fixed value
----------------	-------------

Number of Epochs	120
Learning rate	0.0001
Batch size	32
Optimizer	Adam
Loss function	categorical crossentropy
Metrics	Accuracy

4.5.2.2. Classification Report

Using the model architecture described in **Table 4.3** we got the following results seen in **Figure 4.8**

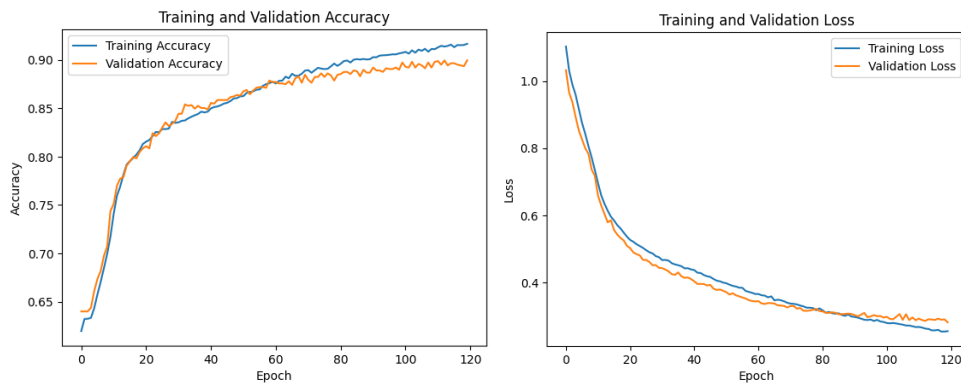


Figure 4.8: Accuracy and Loss graphs for four class classification

As can be seen the training and validation accuracy graph exhibit a noticeable upward trend, indicating positive learning progress, while the loss graph indicates a consistent downward trend, indicating effective convergence during training.

Further information is found from the confusion matrix in **Figure 4.9**:

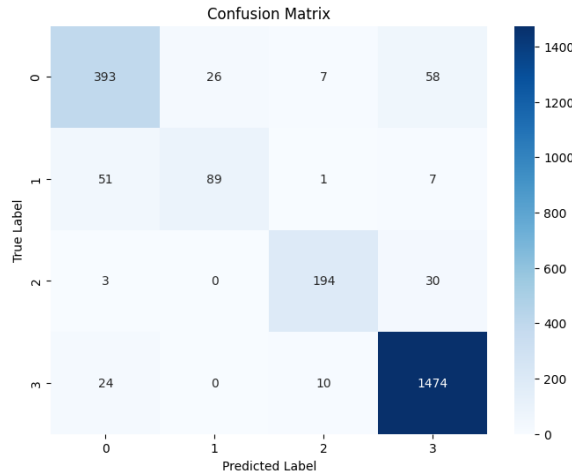


Figure 4.9: Confusion matrix for the four class classification

The confusion matrix in **Figure 4.9** shows that it is easier to detect the No-Anomaly PV modules than the other three Anomaly classes. The false prediction of the No-Anomaly module is mostly on the Cell class. The Cell and Cracking classes are the most false prediction on each other. The Cracking class was the most difficult to be correctly classified comparing to the other classes.

More information are mentioned in **Table 4.8**:

Table 4.8: Performance Metrics for the four class classification

Class	precision	Recall	F1-Score	Total Accuracy
Cell	0.83	0.81	0.82	0.91
Cracking	0.77	0.60	0.68	
Diode	0.92	0.85	0.88	
No-Anomaly	0.94	0.98	0.96	

The reduction to the four classes showed a high impact in the performance of the automatic classifier that achieved up to 91% accuracy. It is concluded from the results that some classes like Hot-Spot and Soiling that have a small and not enough samples can have a huge impact on the efficiency, also that some classes that have similar features can reduce and mislead the classifier so it is for the better to merge the classes that are similar and remove the minority classes.

4.6. Comparison

Automated fault classification in photovoltaic modules is critical for maintaining optimal energy production and system reliability. Convolutional Neural Networks (CNNs) have emerged as powerful tools for this task with their ability to capture patterns in image data. The purpose of this literature review is to compare the findings of this thesis work with those of a relevant paper by Ricardo Henrique Fonseca Alves [47].

Both studies utilized the Infrared Solar Modules dataset. The proposed model achieved an accuracy of 91% for binary classification and a 74% for the twelve-class classification and 91% for the four-class classification after merging some classes that have similar patterns and deleting the minority classes that affected the total accuracy which gave us an improvement and a good result. In contrast, the paper reported accuracies of 92% and 66% for the binary classification and eleven-class classification and an efficiency of 78% for eight-class classification after deleting some of the minority classes.

The differences in accuracy between the proposed model and that of the paper may be attributed to the model architectures and the training procedures.

The approach demonstrated a higher accuracy in the multi-class classification task and outperformed the result of Alves.

Also the strategy of merging and deleting some cases enhanced the quality of the data and increased the accuracy and by comparing it with the eight-class classification where only deleting some classes was considered and only 78% accuracy was achieved, it is clear that it was more efficient.

4.7. Conclusion

In conclusion, this chapter has presented an analysis of binary and multi-class PV module defects image classification using a CNN model using the Infrared Solar Modules dataset. The findings confirmed the significance of model selection in achieving accurate and reliable PV fault detection and classification.

General Conclusion

The work presented in this dissertation underscores the pivotal role of advanced machine learning techniques in enhancing the reliability and efficiency of photovoltaic systems. By integrating infrared thermography with convolutional and artificial neural networks, the proposed method successfully addresses the critical need for rapid and accurate fault detection and classification in PV modules. The empirical results, demonstrating high accuracy in anomaly detection and classification, validate the effectiveness of the approach and highlight its potential for real-world application in large-scale solar plants.

This study contributes to the ongoing efforts to improve the operational efficiency and sustainability of renewable energy systems by ensuring timely identification and rectification of faults. The methodology not only extends the lifespan of PV modules but also optimizes their performance, thereby reducing energy losses and maintenance costs. The findings pave the way for further research and development in the field of automated fault detection, offering a robust foundation for future innovations in solar energy technology.

This proposed method that provides a 91%, 91% and 74% accuracy on the classification of 2-class, 4-class and 12- class, respectively. The easy class prediction modules are on the No-anomaly and Diode modules. The difficult prediction modules are Soiling, Cell-Multi modules, Hot-Spot, Hot-Spot-Multi, Diode-Multi and Vegetation which are the classes that have the least number of samples.

In conclusion, the integration of advanced imaging techniques and machine learning algorithms presents a promising avenue for enhancing the reliability of PV systems. As the demand for clean and sustainable energy continues to grow, such innovations will be instrumental in meeting global energy needs while minimizing environmental impact. The advancements outlined in this thesis represent a significant step forward in the pursuit of more efficient and resilient renewable energy infrastructures.

References:

- [1] B. Reeves, *Solar power DIY handbook: so, you want to connect your off-grid solar panel to a 12 volts battery?* Revisa Publishing Llc, 2018.
- [2] I. Yahyaoui, *Advances in Renewable Energies and Power Technologies*. Elsevier, 2018.
- [3] Stefan, *Solar Electric Power Generation - Photovoltaic Energy Systems*. Springer Science & Business Media, 2007.
- [4] E. Lorenzo, L. AraújoG., P. Davies, Institute Of Solar Energy (Madrid, and E. Al, *Solar electricity : engineering of photovoltaic systems*. Sevilla: Progensa, Cop, 1994.
- [5] B. Sudimac, A. Ugrinović, and M. Jurčević. " *The application of photovoltaic systems in sacred buildings for the purpose of electric power production: The case study of the Cathedral of St. Michael the Archangel in Belgrade*". Sustainability, vol 12,no 4,pp-1408,2020.
- [6] ED Franklin, "Solar Photovoltaic PV System Components", University of Arizona College of agriculture cooperative extension, May2018.
- [7] Yunus Emre Yağan , Kadir Vardar, Mehmet Ali Ebeoğlu, *Modeling and Simulation of PV Systems*,13, 2 Ver. III, Apr 2018.
- [8] A. Algaddafi, et al. "Comparing the impact of the OFF-Grid system and ON-Grid system on a realistic load", 32nd European Photovoltaic Solar Energy Conference and Exhibition, Munich, German, 2016
- [9] S. Lozanova, "Common Solar Panel Defects," *GreenLancer*, Nov. 23, 2023. <https://www.greenlancer.com/post/common-solar-panel-defects#> (accessed may. 28, 2024).
- [10] Admin, "How Does Shading Effect Solar Panels?," *Deege Solar*, Sep. 14, 2021. https://www.deegesolar.co.uk/solar_panels_shading/ (accessed jun. 03, 2024).
- [11] D. Gfeller, R. Neukomm, and U. Muntwyler, "The Bypass Diode – A Weakness in today's PV Systems," 20th European Photovoltaic Solar Energy Conference and Exhibition (EU PVSEC), pp. 1-6, Jun. 2024. doi: <https://doi.org/10.24451/arbor.13941>
- [12] S. AlZahrani, Experimental investigation of soiling impact on PV module performance in Yanbu Al Sinaiyah, Saudi Arabia, Vol 216, November 2023.
- [13] R. Lipták and I. Bodnár, "Simulation of fault detection in photovoltaic arrays," *Analecta Technica Szegedinensia*, vol. 15, no. 2, pp. 31–40, Dec. 2021, doi:

<https://doi.org/10.14232/analecta.2021.2.31-40>

[14] C. Strobl and P. Meckler, “Arc Faults in Photovoltaic Systems,” Oct. 2010, doi: <https://doi.org/10.1109/holm.2010.5619538>.

[15] C. E. Packard, J. H. Wohlgemuth, and S. R. Kurtz, “Development of a Visual Inspection Checklist for Evaluation of Fielded PV Module Condition,” Jan. 2012.

[16] L. Li, Z. Wang, and T. Zhang, “GBH-YOLOv5: Ghost Convolution with BottleneckCSP and Tiny Target Prediction Head Incorporating YOLOv5 for PV Panel Defect Detection,” *Electronics*, vol. 12, no. 3, p. 561, Jan. 2023, doi: <https://doi.org/10.3390/electronics12030561>.

[17] P. Lin, Y. Lin, Z. Chen, L. Wu, L. Chen, and S. Cheng, “A Density Peak-Based Clustering Approach for Fault Diagnosis of Photovoltaic Arrays,” *International Journal of Photoenergy*, vol. 2017, pp. 1–14, 2017, doi: <https://doi.org/10.1155/2017/4903613>.

[18] A. Chouder and S. Silvestre, “Automatic supervision and fault detection of PV systems based on power losses analysis,” *Energy Conversion and Management*, vol. 51, no. 10, pp. 1929–1937, Oct. 2010, doi: <https://doi.org/10.1016/j.enconman.2010.02.025>.

[19] Ball, G., Brooks, B., Johnson, J., Flicker, J., Rosenthal, A., Wiles, J., Sherwood, L., Albers, M., Zgonena, T, “Inverter ground-fault detection ‘blind spot’ and mitigation methods”, Solar Amer., Board Codes Stand. 2013

[20] “Machine Learning and Better Decision Making,” *Rewise*, Feb. 10, 2023. <https://www.rewiseglobal.com/opinion-mining-through-text-analysis> (accessed apr. 17, 2024).

[21] Javatpoint, “Supervised Machine learning - Javatpoint,” *www.javatpoint.com*, 2022. <https://www.javatpoint.com/supervised-machine-learning> (accessed may.05, 2024)

[22] “Unsupervised Machine learning - Javatpoint,” *www.javatpoint.com*. <https://www.javatpoint.com/unsupervised-machine-learning> (accessed may.05, 2024)

[23] P. P. Dec 16 and Read □ □ < ◇2022 6 M., “What is Semi-Supervised Learning? A Guide for Beginners,” *Roboflow Blog*, Dec. 16, 2022. <https://blog.roboflow.com/what-is-semi-supervised-learning/> (accessed may.05, 2024)

[24] K. Suzuki, Ed., ‘Artificial Neural Networks - Methodological Advances and Biomedical

Applications'. InTech, Apr. 11, 2011. doi: 10.5772/644.

[25] N. S. Chauhan, "Loss Functions in Neural Networks," *The AI dream*, Aug. 02, 2021. <https://www.theaidream.com/post/loss-functions-in-neural-networks> (accessed may.11, 2024)

[26] "Gradient Descent algorithm and its variants," *GeeksforGeeks*, Feb. 06, 2019. <https://www.geeksforgeeks.org/gradient-descent-algorithm-and-its-variants/> (accessed may.11, 2024)

[27] F. Schilling, 'The Effect of Batch Normalization on Deep Convolutional Neural Networks', Dissertation, 2016.

[28] R. Sharma, "Deep Learning Activation Functions & their mathematical implementation.," *Nerd For Tech*, May 25, 2021. <https://medium.com/nerd-for-tech/deep-learning-activation-functions-their-mathematical-implementation-b620d536d39b> (accessed may.11, 2024)

[29] X. Xiao and K. Li, "Multi-Label Classification for Power Quality Disturbances by Integrated Deep Learning," *IEEE Access*, vol. 9, pp. 152250–152260, 2021, doi: <https://doi.org/10.1109/access.2021.3124511>. (accessed may. 11, 2024)

[30] C. C. Aggarwal, *Neural Networks and Deep Learning*. Springer Nature, 2023.

[31] S. Mudadla, "What is Learning Rate?," *Medium*, Dec. 07, 2023. <https://medium.com/@sujathamudadla1213/what-is-learning-rate-92d300b347ca> (accessed may. 15, 2024)

[32] "Epochs, Batch Size, Iterations - How they are Important," *www.sabrepc.com*. <https://www.sabrepc.com/blog/Deep-Learning-and-AI/Epochs-Batch-Size-Iterations> (accessed may. 15, 2024)

[33] Y. Chandola, et al, "*Deep learning for chest radiographs: Computer-aided classification*", Elsevier, 2021.

[34] "Evaluation Metrics," *DeepAI*, May 17, 2019. <https://deepai.org/machine-learning-glossary-and-terms/evaluation-metrics> (accessed may. 21, 2024)

[35] S. Sharma, S. Sharma, and A. Athaiya, "Activation Functions in Neural Networks," *International Journal of Engineering Applied Sciences and Technology*, vol. 04, no. 12, pp. 310–316, May 2020, doi: <https://doi.org/10.33564/ijeast.2020.v04i12.054>.

[36] "CS231n Convolutional Neural Networks for Visual Recognition," *Github.io*, 2012. <https://cs231n.github.io/convolutional-networks/> (accessed may. 21, 2024)

- [37] R. Yamashita, M. Nishio, R. K. G. Do, and K. Togashi, “Convolutional Neural networks: an Overview and Application in Radiology,” *Insights into Imaging*, vol. 9, no. 4, pp. 611–629, Jun. 2018, doi: <https://doi.org/10.1007/s13244-018-0639-9>. (accessed may. 21, 2024)
- [38] GeeksforGeeks, “CNN | Introduction to Pooling Layer,” *GeeksforGeeks*, Aug. 05, 2019. <https://www.geeksforgeeks.org/cnn-introduction-to-pooling-layer/> (accessed may. 21, 2024)
- [39] A. Ghosh, et al. ‘Fundamental Concepts of Convolutional Neural Network’, IEEE, transaction of Biomedical Engineering, 2020
- [40] Matthew M, Edward O, Nikhil V. Infrared solar module dataset for anomaly detection. ICLR 2020.
- [41] Ç. Uslu, “What is Kaggle?,” *www.datacamp.com*, Mar. 2022. <https://www.datacamp.com/blog/what-is-kaggle> (accessed may. 31, 2024)
- [42] Python Software Foundation, “What Is Python? Executive Summary,” *Python*. <https://www.python.org/doc/essays/blurb/> (accessed may. 31, 2024)
- [43] “TensorFlow,” *TensorFlow*. <https://www.tensorflow.org/?hl=fr>
- [44] Keras, “Home - Keras Documentation,” *Keras.io*, 2019. <https://keras.io/>
- [45] “Accuracy vs. precision vs. recall in machine learning: what’s the difference?,” *www.evidentlyai.com*. <https://www.evidentlyai.com/classification-metrics/accuracy-precision-recall> (accessed jun. 03, 2024)
- [46] “What is the F1-score?,” *Educative: Interactive Courses for Software Developers*. <https://www.educative.io/answers/what-is-the-f1-score> (accessed jun. 03, 2024)
- [47] R. Alves, et al, “fault classification in photovoltaic modules using Convolutional Neural Networks”, *Renewable Energy*, Vol 179, 2021, Pp 502-516.